

See discussions, stats, and author profiles for this publication at: <https://www.researchgate.net/publication/228328200>

Peer Reviewed: SPR of Ultrathin Organic Films

ARTICLE *in* ANALYTICAL CHEMISTRY · JUNE 1998

Impact Factor: 5.64 · DOI: 10.1021/ac981909r

CITATIONS

102

READS

46

2 AUTHORS, INCLUDING:



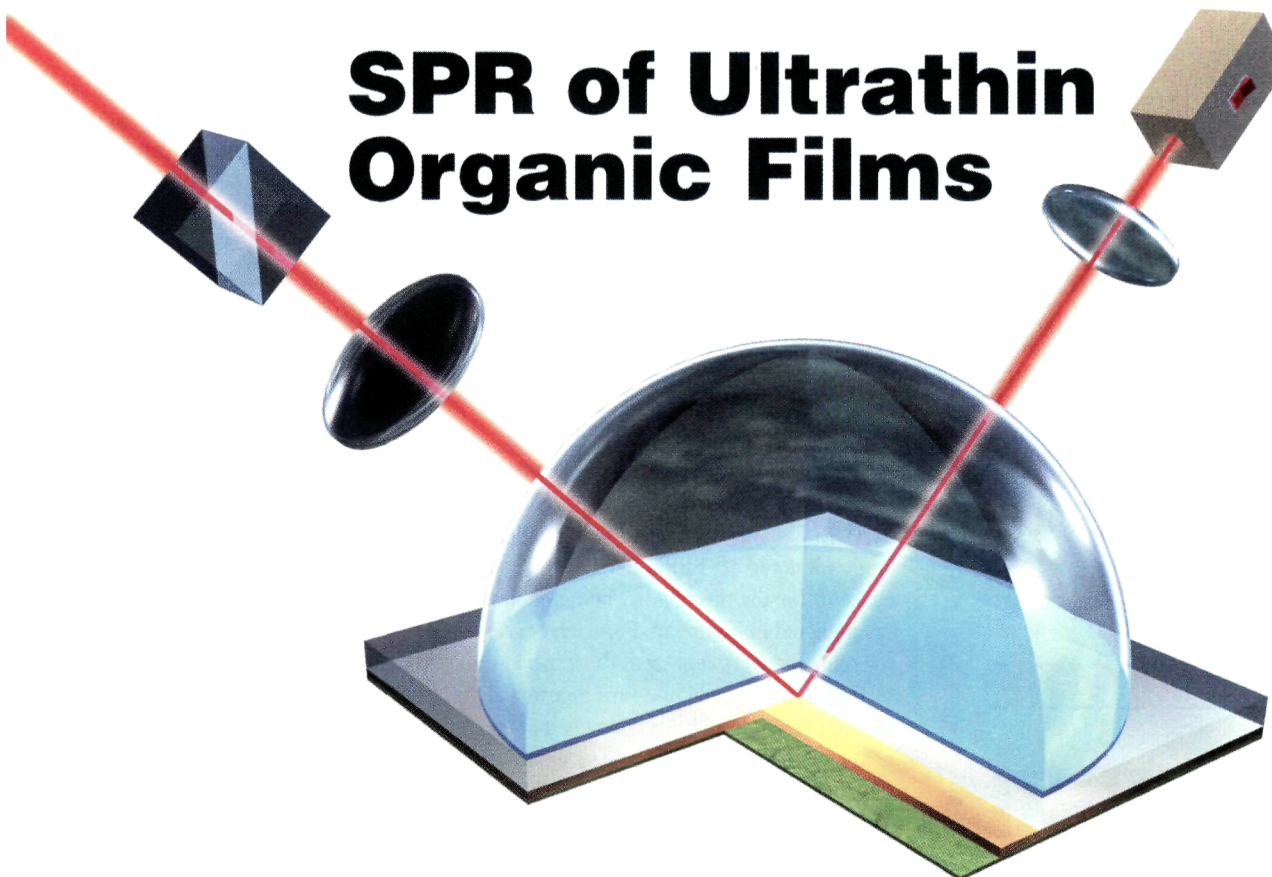
[Robert Corn](#)

University of California, Irvine

193 PUBLICATIONS 10,607 CITATIONS

[SEE PROFILE](#)

SPR of Ultrathin Organic Films



Surface plasmon resonance (SPR) methods are surface-sensitive spectroscopic techniques that can be used to characterize a variety of ultrathin organic monolayers and multilayers at gold, silver, and copper surfaces. For example, SPR measurements have been used to study Langmuir–Blodgett films (1–3), self-assembled organic monolayers (4, 5), specifically and nonspecifically adsorbed biopolymers (including DNA) (6–13), nonlinear optical thin films (14), and thin organic films at electrochemical interfaces (15, 16).

SPR methods have been used to enhance fluorescence (17, 18), Raman scattering (18–22), and optical second harmonic generation at metal/dielectric interfaces (23, 24), but in their simplest form, SPR measurements are used to monitor the changes in thickness or index of refraction of ultrathin organic films at metal sur-

Measurements by surface plasmon resonance monitor changes in thickness or the index of refraction of ultrathin organic films on metal surfaces.

faces. In this respect, SPR measurements are similar to ellipsometry (25) except that the two methods have different degrees of surface specificity and sensitivity. The SPR index of refraction measurement is the basis of the recently introduced BIACORE SPR adsorption instrument (1, 26).

In this Report, three different examples of how SPR techniques can be applied to

studying ultrathin organic films are discussed (Figure 1). In Figure 1a, SPR scanning and imaging measurements are used to study protein adsorption onto chemically modified gold surfaces. In Figure 1b, SPR imaging measurements are used to follow the sequential hybridization adsorption of DNA molecules. In Figure 1c, the electrostatic fields inside a noncentrosymmetric zirconium phosphonate film incorporated into an electrochemical interface are measured with electrochemically modulated SPR methods.

Scanning-angle measurements

Briefly stated, the surface selectivity of SPR arises from the enhancement of the optical electric fields at metal surfaces when surface plasmon polaritons (SPPs) are created at the metal/dielectric interface. SPPs are coupled photon–plasmon surface electromagnetic waves that propagate parallel to the metal/dielectric interface. The intensity of the optical electric fields associated with an SPP decays exponentially away from the metal surface. The key point is that a typi-

Anthony G. Frutos

Robert M. Corn

University of Wisconsin–Madison

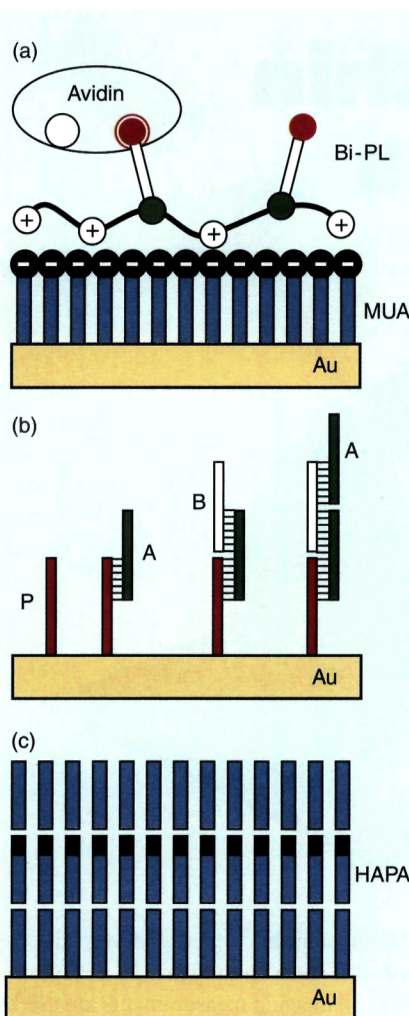


Figure 1. Examples of surface chemistries characterized by SPR.

(a) The specific adsorption of the protein avidin onto a gold surface modified with a monolayer of MUA onto which a monolayer of biotinylated poly-L-lysine (bi-PL) has been electrostatically adsorbed. (b) The sequential hybridization of DNA target molecules A and B to the surface-bound DNA probe molecule P is monitored with SPR imaging. (c) The noncentrosymmetric molecule HAPA can be used to probe the electric fields inside organic multilayer films in an electrochemical environment using electrochemically modulated SPR methods.

cal decay length for an SPP into the dielectric is on the order of 200 nm. Unfortunately, SPPs cannot be created on an isolated planar metal surface (either bare or coated). Instead, a prism or grating coupling geometry is typically used to excite SPPs (27). One such geometry, the Kretschmann prism coupling configuration, is shown schematically in Figure 2.

In an SPR scanning experiment, the

reflectivity of a 1-mW p-polarized (i.e., polarized parallel to the plane of incidence) HeNe laser (632.8 nm) is measured as a function of incident angle from a prism-sample assembly as shown in Figure 2. The sample consists of an organic thin film adsorbed onto a 47-nm gold film that has been vapor deposited onto a glass microscope slide cover. The sample is brought into optical contact with the BK7 glass prism using a thin layer of index-matching fluid such as ethylene glycol. The prism-sample assembly is mounted onto a rotation stage, which allows scanning of the incident angle with a resolution of 0.004°.

Figure 3a displays the percent reflectivity (% R) obtained as a function of incident angle (denoted as "SPR reflectivity curves") for a series of adsorbed monolayers depicted in Figure 1a. For each curve, the open markers represent the experimental data, and the solid lines are theoretical calculations of the SPR reflectivity curves using a four-phase (BK7/gold/organic film/air) complex Fresnel calculation. These calculations were performed using the N-phase method as detailed by Hansen (28), and the details of our specific implementation can be found elsewhere (29; see also <http://cornifo.chem.wisc.edu/calculations.html>). Notice the excellent

agreement between theory and experimental data.

The SPR reflectivity curves have several distinct features. At an angle of approximately 41.3°, a cusp in the reflectivity curves is observed, which is caused by the critical angle for the BK7 prism (refractive index $n_{BK7} = 1.515$). The position of this cusp does not change with the presence of monolayers on the gold film, and is used to ensure a reproducible calibration of the incident angle. Beyond the critical angle, a minimum in the reflectivity is observed, with the reflectivity plunging dramatically from greater than 90% to less than 1%. This drop is the well-documented creation of SPPs at the gold/thin film interface, and the angle of minimum reflectivity is denoted as the "SPR angle".

The sharpness of the SPR minimum allows for a very accurate determination of the position of the SPR angle. At the reflectivity minimum, the light waves in the prism are coupled to the surface plasmons at the gold/thin film interface. Because the optical electric fields are localized to within ~200 nm from the gold surface, the position of the SPR angle is extremely sensitive to the index of refraction (n) of the adjacent medium.

Figure 3b shows an expanded view of the curves near the reflectivity minimum.

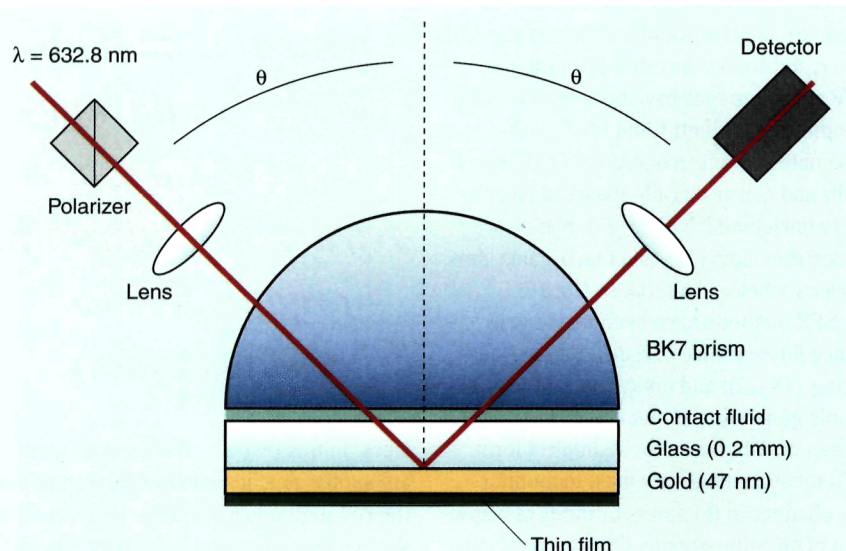


Figure 2. Prism-sample assembly for an SPR scanning-angle instrument.

The reflectivity of a 1-mW HeNe laser as a function of incident angle is measured from a prism-sample assembly. The sample is an organic thin film adsorbed onto gold film that has been vapor deposited onto a glass microscope slide cover. The sample is brought into optical contact with the prism using a thin layer of index-matching fluid. (Adapted from Ref. 8.)

Notice the significant shift in the minimum for just one monolayer of adsorbed material. The magnitude of this shift in the SPR angle ($\Delta\theta$) depends upon the thickness of the monolayer and n of the adsorbed molecules at 632.8 nm. Thus, the thickness of a monolayer can be obtained by measuring the SPR angle before and after adsorption, provided n is known. Though usually estimated from bulk indices of refraction, n of the monolayer can, in some instances, be extracted by measuring SPR curves at a number of wavelengths (30).

In Figure 3, the open circles represent the data from a clean gold surface, and the open triangles show the data from the same surface after the adsorption of a monolayer of the alkanethiol 11-mercaptoundecanoic acid (MUA). The adsorption of the MUA monolayer resulted in a shift in the SPR angle of $0.179 \pm 0.009^\circ$ from the bare gold surface. Using a four-phase (BK7/gold/MUA/air) complex Fresnel calculation, $\Delta\theta$ was converted to a thickness of $17.0 \pm 0.9 \text{ \AA}$ by assuming $n_{\text{MUA}} = 1.45$ (31). This film thickness is in excellent agreement with previous ellipsometric film thickness measurements of $16\text{--}19 \text{ \AA}$ for the MUA monolayer (31) and confirms the accuracy of the SPR technique.

SPR measurements can be performed in an ex situ or in situ configuration. To monitor rapid changes in adsorption, the incident HeNe laser can be focused onto the sample, and a spread of angles can be monitored simultaneously (1, 32). However, it is more difficult to extract quantitative thickness information if only a small portion of the SPR reflectivity curve is measured (33).

The adsorption of two additional biopolymer monolayers onto this MUA-modified gold surface has also been monitored with the scanning SPR technique (34). We have shown that the specific adsorption of the protein avidin onto gold surfaces can be controlled with monolayers of the polypeptide poly-L-lysine (PL) modified with biotin. Avidin is a tetrameric glycoprotein that contains four specific binding sites for the small molecule biotin. Upon the electrostatic adsorption of a monolayer of biotinylated PL (bi-PL) to the MUA monolayer, an additional shift in the SPR angle of 0.205° was observed, corresponding to a bi-PL thickness of 17.0 \AA .

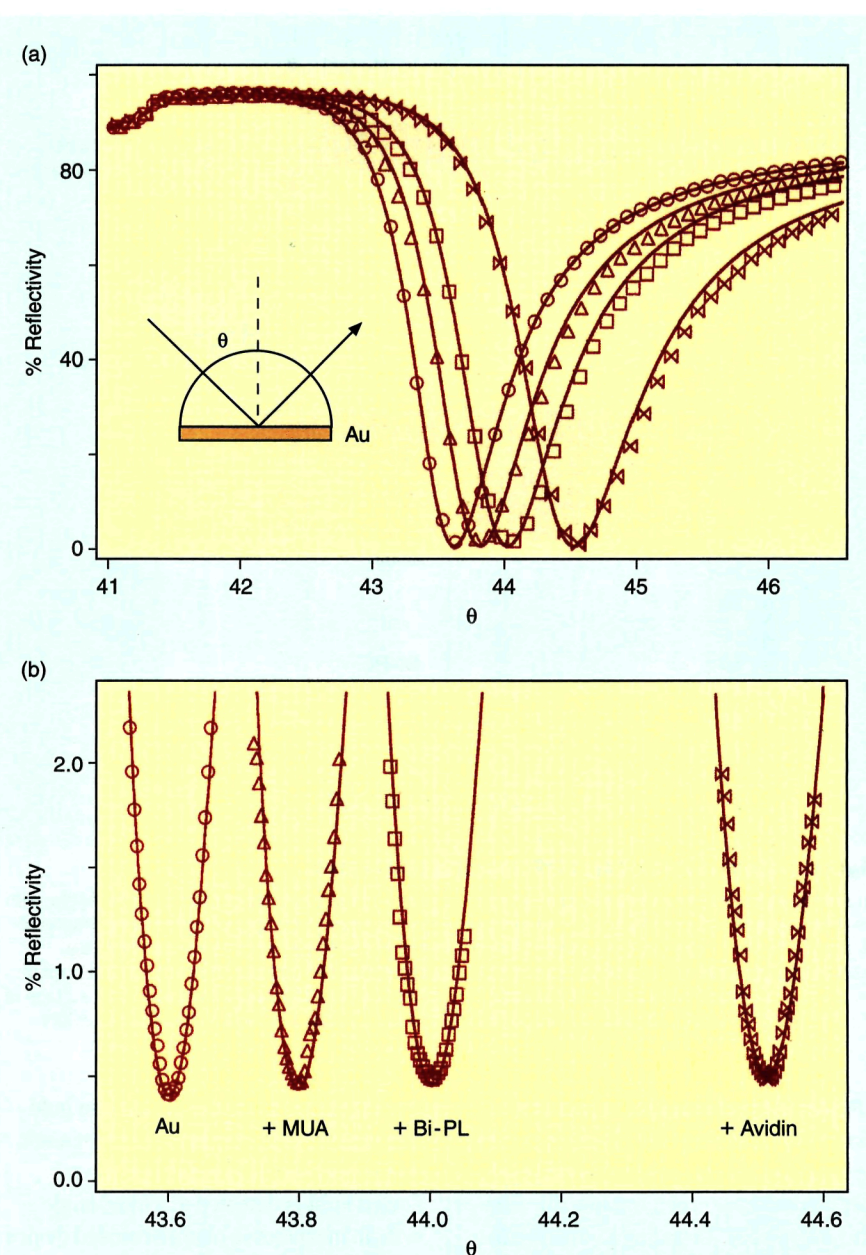


Figure 3. Reflectivity curves.

(a) The SPR reflectivity curves for a clean gold surface (\circ) and the same surface after the sequential adsorption of an MUA monolayer (\triangle), a bi-PL monolayer (\square), and a layer of the protein avidin (\times). (b) An expanded view of the SPR curves for the same sample as in (a) near the reflectivity minimum. The shift in the angle of minimum reflectivity, denoted as θ_{sp} , upon the adsorption of material is used to determine the thickness of the adsorbed layer via complex Fresnel calculations (solid lines). (Adapted from Ref. 34.)

The biotin moieties attached to the surface via PL act as specific adsorption sites for avidin, and upon exposure of the gold/MUA/bi-PL surface to an avidin solution, an additional shift of 0.485° corresponding to an avidin layer thickness of 41.0 \AA was observed. This is in good agreement with the expected thickness

for a packed monolayer of avidin. No avidin adsorption occurred onto a PL monolayer that had not been biotinylated, indicating that the avidin was specifically adsorbed to the biotin sites. The preferential adsorption of avidin to bi-PL over PL was investigated further using SPR imaging measurements.

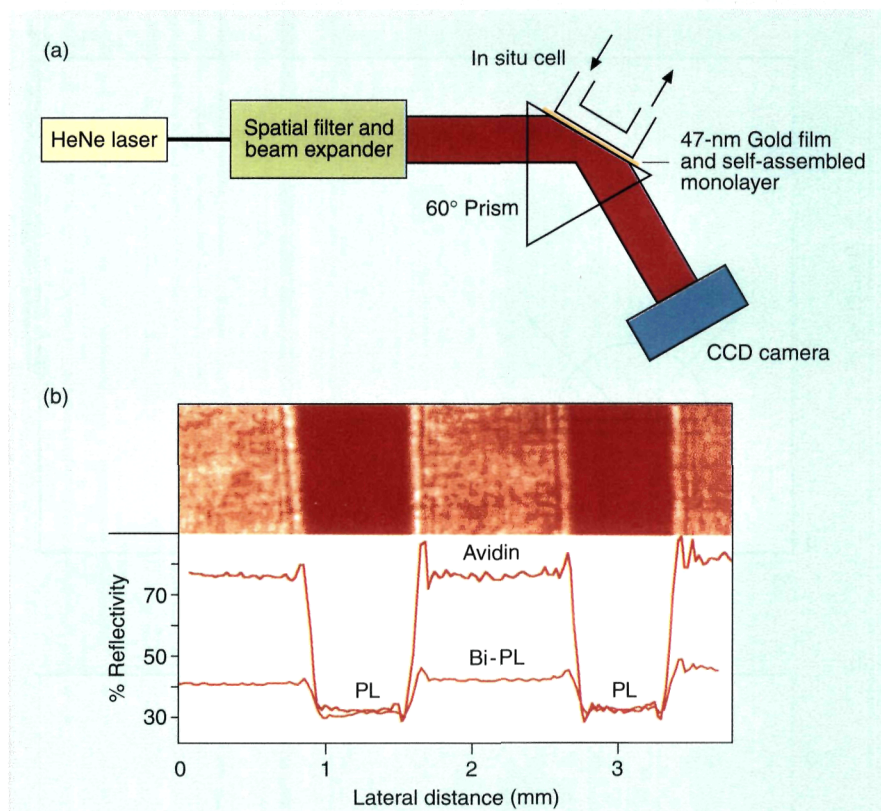


Figure 4. Schematic of an SPR imaging apparatus.

(a) An expanded HeNe laser beam is incident on a prism-sample assembly near the SPR angle, with the reflected light detected by a CCD camera. (b) A gold surface patterned with alternating stripes of PL and bi-PL was exposed to a solution of avidin to obtain the image, which was quantitatively analyzed by generating line profiles across it by averaging the %R values measured at each pixel of the charge-coupled device across the stripes. The lower line was obtained from the original surface of MUA/PL and MUA/bi-PL stripes. The upper line was obtained after exposing the surface to avidin.

SPR imaging measurements

Along with scanning SPR, fixed-angle SPR imaging can also be used to measure adsorption onto patterned organic thin films. The ability of SPR imaging to observe patterned surfaces (35–38) makes this technique ideally suited for biosensor applications, which often require monitoring simultaneous adsorption onto many surface functionalities. For example, SPR imaging experiments that use two functionalized surfaces placed on the same substrate and exposed to identical conditions can be used to perform very accurate differential biopolymer adsorption studies. This methodology can also be used to identify and discriminate against any nonspecific adsorption processes.

A schematic diagram of an SPR imaging apparatus is shown in Figure 4a. In this experiment, an expanded HeNe laser beam

is used to illuminate the prism-thin gold film sample assembly at an incident angle that is near the SPR angle, and the reflected light is detected at a fixed angle with an inexpensive charge-coupled device (CCD) camera to produce an “SPR image” such as the one shown in Figure 4b. This image arises from variations in the reflected light intensity from different parts of the sample; these variations are created by changes in the organic thin-film thickness or in n that occur upon adsorption onto the modified gold surface.

By creating patterns of two different alkanethiol self-assembled monolayers on a single thin gold film, a differential adsorption measurement can be performed. These differential adsorption measurements are comparable in sensitivity to the SPR angle shift measurements of biopolymer adsorption described previously with

the scanning SPR instrument. As with the SPR scanning-angle technique, the SPR imaging technique can be used to monitor the adsorption of submonolayer amounts of material in both ex situ and in situ configurations.

To make differential adsorption measurements with the SPR imaging apparatus, surfaces with alternating stripes of two different surface functional groups are created. These surfaces are prepared by a series of adsorption or self-assembly, photochemical desorption, and rinsing steps. The preferential adsorption of avidin onto bi-PL versus unmodified PL is demonstrated in the SPR imaging experiment shown in Figure 4. A gold surface was prepared with the alternating stripes of bi-PL and PL (6). First, the entire surface was covered with MUA and bi-PL. Stripes of the MUA/bi-PL were then removed by irradiating the surface with UV light through a mask and then rinsing with ethanol and water. The sample was immersed into an MUA solution to refill those areas just removed, and these newly deposited MUA stripes were coated with PL by immersing the sample into a PL solution. When the reflectivity from such a surface is measured in an SPR imaging experiment at a fixed angle, images of the type shown in Figure 4 are obtained.

The SPR image from a two-component surface can be analyzed quantitatively by generating a “line profile” across the image by averaging the %R values measured at each pixel of the CCD camera along the stripes. Figure 4 shows two of these line profiles; the lower line was obtained from the original surface of MUA/PL and MUA/bi-PL stripes. Notice the 10% difference in the reflectivity between the two regions, which results because the bi-PL monolayer is 6.5 Å thicker than the unmodified PL.

After exposing the surface to avidin, a second line profile (upper line) shows that the reflectivity increased from 40% to 80% in the bi-PL regions but not at all on the PL-covered stripes. The increase in reflectivity for the bi-PL-coated stripes results from a shift in the SPR angle caused by the adsorption of a 40 Å layer of avidin. Conversely, the lack of change in reflectivity for the PL stripes indicates no avidin adsorption occurred onto those regions. Fig-

ure 4 also displays the SPR image of these alternating stripes of MUA/PL (dark regions) and MUA/bi-PL/avidin (light regions). The SPR image and line profiles data clearly demonstrate that the avidin specifically adsorbs to the biotin moieties of the bi-PL, and that unmodified PL prevents the nonspecific adsorption of avidin onto the metal surface.

Although in principle this information could have been obtained from a series of scanning SPR measurements, the SPR imaging technique is a rapid and very sensitive method for studying protein adsorption. The speed and sensitivity of these experiments arise because adsorption onto a single surface containing multiple areas with different functional groups can be measured simultaneously and because each functional group is exposed to identical adsorption conditions. Very small changes in %R corresponding to sub-monolayer amounts of biopolymer adsorption can be observed with this measurement, and if the data are normalized (as in Figure 4) to obtain quantitative %R values, an effective average thickness can be determined.

In a second example of the SPR imaging experiment, the technique was used to detect the presence of a specific DNA sequence in solution by hybridization adsorption onto an array of immobilized DNA probes. The rapid assay of mixtures of DNA sequences from solution by hybridization adsorption has been studied extensively in recent years for both genetic analysis and DNA sequencing applications. The SPR imaging geometry allows us to measure, in an *in situ* environment, the simultaneous hybridization adsorption of unlabeled oligonucleotides onto an array of immobilized oligonucleotides.

In this SPR imaging experiment, two different DNA "probe" molecules (P1 and P2) each composed of 30 nucleotides were covalently bound to distinct spots on a modified gold surface in the manner shown in the inset in Figure 5. The adsorption of a DNA "target" molecule (target A) that was complementary to the surface-bound probe molecule P2 was monitored, with P1 being used to verify the specificity of the surface hybridization. Figure 5 shows the line profiles from the *in situ* SPR imaging experiment. The curve labeled P in Figure 5 is a

line profile taken through the two spots prior to hybridization, as shown by the dotted line in the inset of the figure.

Note that the two DNA probe spots are clearly visible in the line profile, in contrast to fluorescence measurements of hybridization adsorption in which only the complementary target strand is detected. When a solution containing target A was injected into the *in situ* cell, a line profile of the resulting image, line A1 in Figure 5, was obtained. It can be seen from line A1 that this complement adsorbs only to the P2 DNA spot, as evidenced by an increase in the reflectivity of the P2 spot and essentially no change in the reflectivity for the P1 spot. This clearly demonstrates the specificity of the surface hybridization adsorption process.

The SPR imaging experiment in Figure 5 was also used to demonstrate the sequential hybridization adsorption of DNA molecules onto the chemically modified gold surface (33). As depicted in Figure 1b, target A (the strand of DNA complementary

to the surface-bound probe P2) was designed so that only half of the 30 bases in the oligonucleotide are involved in hybridization to the surface probe. The remaining free bases were used to hybridize a layer of a second 30-base oligonucleotide, target B, to the surface. Target B was, in turn, designed such that it was able to hybridize a second layer of target A. By sequentially exposing the surface to solutions of first target A, and then target B, it was possible to perform multiple hybridizations to a single strand of probe DNA using only two different target oligonucleotides.

Figure 5 shows the line profiles from an *in situ* SPR imaging experiment in which multiple hybridizations were used to amplify the SPR signal produced by the initial covalently bound probe DNA. Following the initial hybridization adsorption step, the sample was exposed to target B and further adsorption onto P2 was observed (line B1). This sequential hybridization was repeated several times to give line profiles labeled A2 through B3. Notice that the increase in

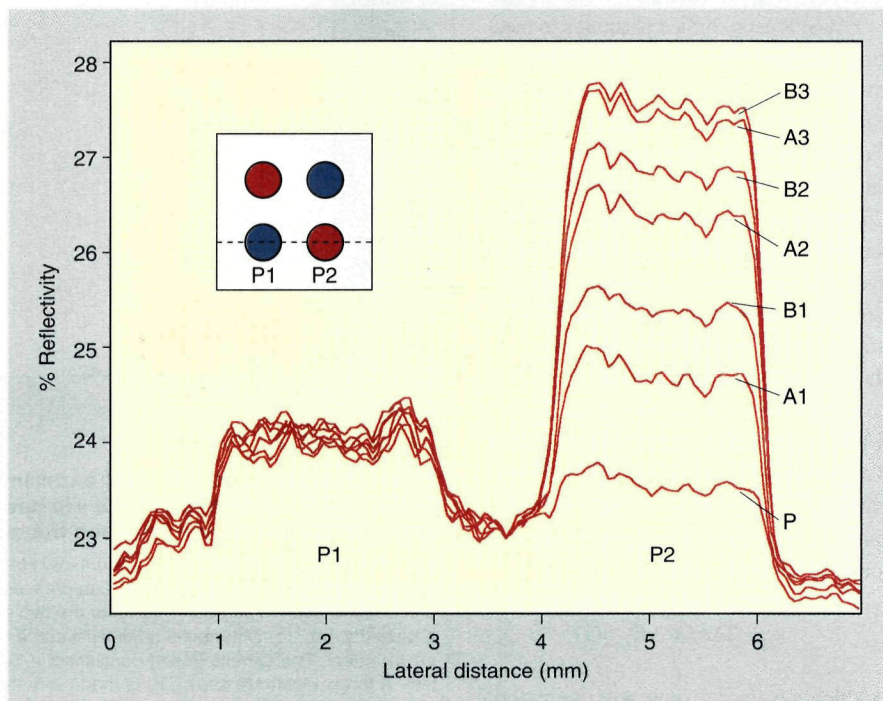


Figure 5. Line profiles from the SPR images of the multiple sequential hybridization of DNA target molecules to surface-bound DNA probe molecules.

DNA probe molecules, P1 and P2, were covalently bound in distinct spots on a modified gold surface. Line profiles from the SPR images of the surface were taken prior to hybridization (line P) and after exposing the surface to DNA target molecules complementary to P2 (line A1). Further hybridizations were performed according to the scheme depicted in Figure 2b to give lines B1 through B3.

%R is not linear, but begins to level out after five hybridization steps. There are two contributions to this behavior: The SPR response is not linear with increasing thickness and hybridization efficiencies of each adsorption step are less than 100%. As a final point, the hybridization adsorption of these DNA molecules onto the modified gold surface was monitored in real time using the SPR imaging technique. Thus, this SPR method can, in principle, also be used to study DNA hybridization adsorption and self-assembly kinetics.

EM-SPR

A recent set of experiments demonstrates how a novel extension of the SPR methodology called electrochemically modulated-SPR (EM-SPR) can be used to monitor electrostatic fields inside organic monolayer and multilayer films. In an electrochemical environment, the strength of the electrostatic fields within the interfacial region of a chemically modified electrode is a fundamental parameter that controls the reactivity of any chemical species incorporated into the thin film.

EM-SPR uses surface plasmons to measure the minute changes in n of a noncentrosymmetric thin organic film that occur when an external electrostatic field is applied. The noncentrosymmetric thin organic film used in the initial set of experiments (15) was a zirconium phosphonate (ZP) multilayer film that contained a single ZP monolayer of the asymmetric nonlinear optical azobenzene chromophore HAPA ([5-[4-[(4-[(6-hydroxyhexyl)sulfonyl]phenyl]azo)phenyl]pentoxy]phosphonic acid).

The change in n (or Δn) of this ZP/HAPA film when an external electric field is applied is referred to as the linear electrooptical effect, and for a nonbirefringent material, is described by the electrooptic coefficient tensor element

$$r_{33} = 2\Delta n/n^3 \Delta E_z \quad (1)$$

in which n is the isotropic n of the material and Δn is the change created by the change in an electric field applied along the z -axis (i.e., perpendicular to the electrode surface), which is ΔE_z . The relationship in Equation 1 is used in two ways: First, the value of r_{33} is determined for an ultrathin

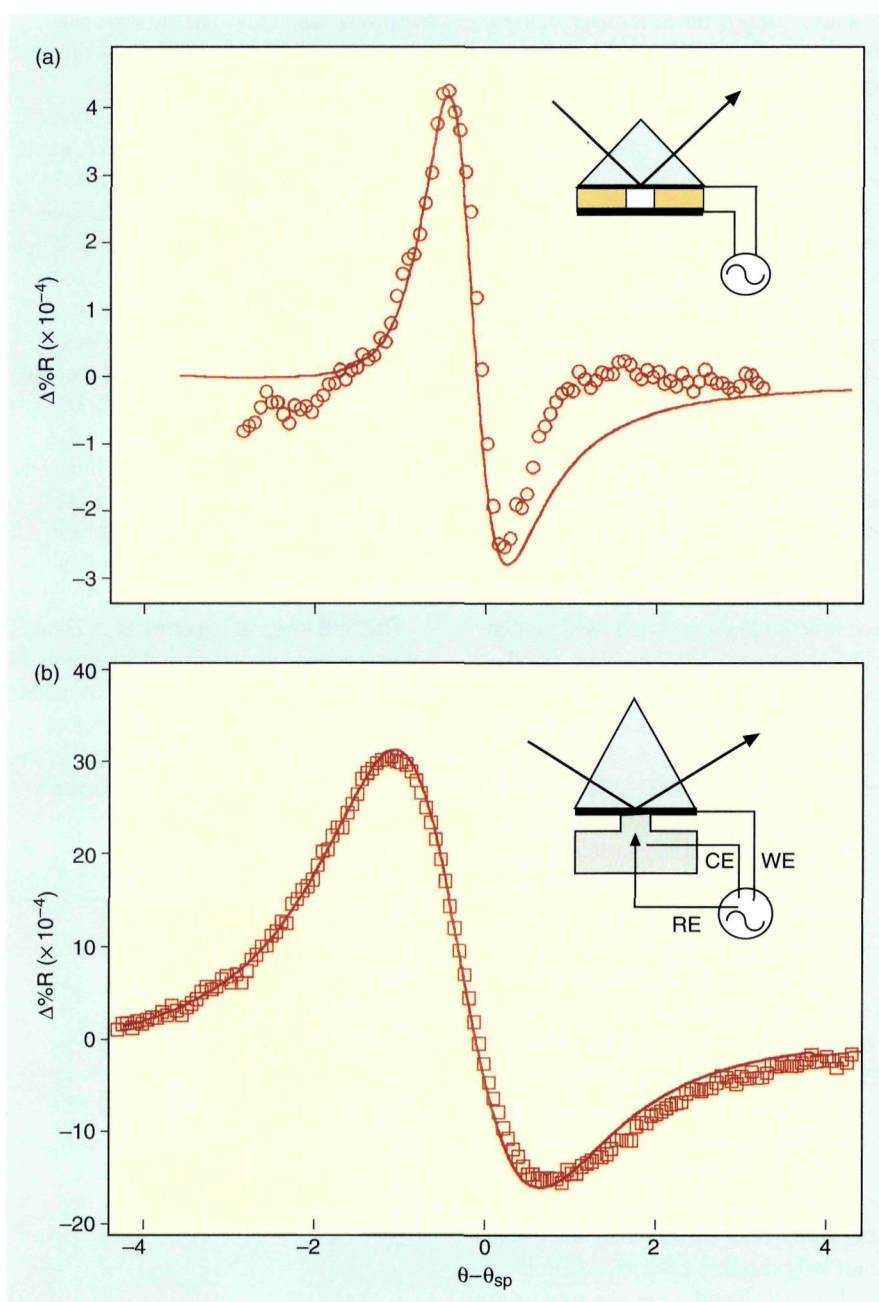


Figure 6. Results for EM-SPR experiments used to measure the electric fields inside a HAPA film. Data are normalized by plotting the angle as $\theta - \theta_{sp}$, which is the difference between the angle of incidence and the SPR angle.

(a) Differential reflectivity curve for a 4.4-nm HAPA film in an air gap capacitor experiment. The sample (inset) consists of thin Mylar film pressed between the ZP-modified gold film and a gold electrode. Electrical contact is made to the two gold surfaces, and a sinusoidal waveform is applied across the gap. (b) Differential reflectivity curve for a 6.7-nm HAPA film in an electrochemical environment. The sample (inset) consists of a Teflon cell pressed against the ZP-modified gold film. A three-electrode assembly is made with the ZP-modified gold film as the working electrode. (Data from Ref. 15.)

noncentrosymmetric ZP/HAPA film by measuring Δn in an air gap capacitor that has a known applied field strength, and then, in a second set of experiments, Δn is measured in an electrochemical environ-

ment. With the previously determined value of r_{33} , the electrostatic field inside the organic thin film can then be estimated from Equation 1. This is an optical measurement of the electrostatic field within

the thin film, and it can be used to probe electric field profiles by moving the position of the HAPA molecules inside the organic multilayer (16).

A modulated SPR experiment is used to measure the field-induced changes in Δn . Surface plasmons are created at a gold/dielectric interface in an EM-SPR experiment with an apparatus similar to that used in the scanning SPR measurement. The small changes in reflectivity that occur upon potential modulation are monitored as a function of incident angle in the region of θ_{sp} . These experimental EM-SPR "differential reflectivity" or " $\Delta\%R$ " curves are modeled with complex Fresnel calculations to relate the measured $\Delta\%R$ to Δn .

Figure 6a plots the differential reflectivity curve measured in an air gap capacitor experiment for a 4.4-nm ZP film that contained one HAPA monolayer. No differential reflectivity response was observed when a completely centrosymmetric film was used; a noncentrosymmetric optical chromophore had to be present in the ZP multilayer. In this experiment, an AC voltage of 30 V at 10 kHz was applied to the sample, and a maximum differential reflectivity of 4×10^{-4} was observed near θ_{sp} . The solid line is the differential reflectivity curve expected for Δn of the HAPA monolayer of 8.0×10^{-6} . From this experiment, an electrooptic coefficient of 11 pm/V was obtained (15).

In Figure 6b the differential reflectivity curve for a 6.7-nm ZP/HAPA film that contained a single HAPA monolayer in an electrochemical environment is plotted. The electrode potential was modulated by 50 mV, and a maximum differential reflectivity of 3×10^{-3} was observed, corresponding to a Δn of 3.3×10^{-5} (as determined from multilayer Fresnel calculations). Note that this maximum differential reflectivity is an order of magnitude greater than in the air gap experiment shown in Figure 6a. Using the electrooptic coefficient of 11 pm/V determined in the air gap experiment, this Δn of 3.3×10^{-5} corresponds to a ΔE_z of 1.4×10^4 V/cm. This number is consistent with the field strength values observed by other groups for monolayer films at electrode surfaces as determined from electrochromic shifts in fluorescence and electroreflectance measurements (39). In another set of measurements, the EM-SPR

technique has been used to measure ΔE_z for various ZP/HAPA films as a function of film thickness and chromophore position inside the multilayer (16).

The EM-SPR technique is an extremely sensitive method for monitoring field-induced changes in the n of ultrathin films in an electrochemical environment, and in the future, should provide detailed information about the electric fields inside other noncentrosymmetric assemblies such as Langmuir-Blodgett films and nonlinear optical polymer films.

The ability of SPR measurements to characterize the adsorption of unlabeled organic molecules and biopolymers onto chemically modified gold surfaces in both ex situ and in situ configurations makes these techniques a very simple yet extremely versatile and sensitive set of optical methods for the study of ultrathin organic films. There are quite a few other SPR techniques, applications, and methodologies, and we refer the reader to some excellent recent reviews (33, 40-42).

We gratefully acknowledge the financial support of the National Science Foundation.

References

- Löfås, S.; Malmqvist, M.; Rönnerberg, I.; Stenberg, E.; Liedberg, B.; Lundström, I. *Sens. Actuators, B* **1991**, 5, 79.
- Lawrence, C. R.; Martin, A. S.; Sambles, J. R. *Thin Solid Films* **1992**, 208, 269.
- Wijekoon, W.M.K.P. et al. *Langmuir* **1992**, 8, 135.
- Peterlinz, K. A.; Georgiadis, R. *Langmuir* **1996**, 12, 4731.
- Lang, H.; Duschl, C.; Gratzel, M.; Vogel, H. *Thin Solid Films* **1992**, 210/211, 818.
- Jordan, C. E.; Corn, R. M. *Anal. Chem.* **1997**, 69, 1449.
- Jordan, C. E.; Frutos, A. G.; Thiel, A. J.; Corn, R. M. *Anal. Chem.* **1997**, 69, 4939.
- Jordan, C. E.; Frey, B. L.; Kornguth, S.; Corn, R. M. *Langmuir* **1994**, 10, 3642.
- Mrksich, M.; Sigal, G. B.; Whitesides, G. M. *Langmuir* **1995**, 11, 4383.
- Peterlinz, K. A.; Georgiadis, R.; Herne, T. M.; Tarlov, M. J. *J. Am. Chem. Soc.* **1997**, 119, 3401.
- Spinke, J.; Liley, M.; Guder, H-J.; Angermaier, L.; Knoll, W. *Langmuir* **1993**, 9, 1821.
- Thiel, A. J.; Frutos, A. G.; Jordan, C. E.; Corn, R. M.; Smith, L. M. *Anal. Chem.* **1997**, 69, 4948.
- Terrettaz, S.; Stora, T.; Duschl, C.; Vogel, H. *Langmuir* **1993**, 9, 1361.
- Hanken, D. G.; Corn, R. M. *Anal. Chem.* **1995**, 67, 3767.
- Hanken, D. G.; Naujok, R. R.; Gray, J. M.; Corn, R. M. *Anal. Chem.* **1997**, 69, 240.
- Hanken, D. G.; Corn, R. M. *Anal. Chem.* **1997**, 69, 3665.
- Kano, H.; Kawata, S. *Opt. Lett.* **1996**, 21, 1848.
- Knobloch, H.; Brunner, H.; Leitner, A.; Aussenegg, F.; Knoll, W. *J. Chem. Phys.* **1993**, 98, 10093.
- Corn, R. M.; Philpott, M. R. *J. Chem. Phys.* **1984**, 80, 5245.
- Knobloch, H.; Duschl, C.; Knoll, W. *J. Chem. Phys.* **1989**, 91, 3810.
- Knoll, W.; Philpott, M. R.; Swalen, J. D.; Girlando, A. *J. Chem. Phys.* **1982**, 77, 2254.
- Pettinger, B.; Tadjeddine, A.; Kolb, D. M. *Chem. Phys. Lett.* **1979**, 66, 544.
- Simon, H. J.; Benner, R. E.; Rako, J. G. *Opt. Commun.* **1977**, 23, 245.
- Corn, R. M.; Romagnoli, M.; Levenson, M. D.; Philpott, M. R. *Chem. Phys. Lett.* **1984**, 106, 30.
- Collins, R. W.; Kim, Y. *Anal. Chem.* **1990**, 62, 887 A.
- Malmqvist, M. *Nature* **1993**, 361, 186.
- Agranovich, V. M.; Mills, D. L. *Surface Polaritons*; North-Holland: Amsterdam, 1982.
- Hansen, W. N. *J. Opt. Soc. Am.* **1968**, 58, 380.
- Campbell, D. J. Ph.D. thesis, University of Wisconsin-Madison, 1990.
- Peterlinz, K. A.; Georgiadis, R. *Opt. Commun.* **1996**, 130, 260.
- Bain, C. D.; Troughton, E. B.; Tao, Y.; Evall, J.; Whitesides, G. M.; Nuzzo, R. G. *J. Am. Chem. Soc.* **1989**, 111, 321.
- Sirila, A. R.; Bohn, P. W. *Langmuir* **1991**, 7, 2188.
- Hanken, D. G.; Jordan, C. E.; Frey, B. L.; Corn, R. M. *Electroanal. Chem.* **1998**, 20, 141.
- Frey, B. L.; Jordan, C. E.; Kornguth, S.; Corn, R. M. *Anal. Chem.* **1995**, 67, 4452.
- Fischer, B.; Heyn, S. P.; Egger, M.; Gaub, H. E. *Langmuir* **1993**, 9, 136.
- Rothenhäusler, B.; Knoll, W. *Nature* **1988**, 332, 615.
- Schmitt, F.-J.; Knoll, W. *Biophys. J.* **1991**, 60, 716.
- Flatgen, G.; Krischer, K.; Pettinger, B.; Doblhofer, K.; Junkes, H.; Ertl, G. *Science* **1995**, 269, 668.
- Pope, J. M.; Tan, Z.; Kimbrell, S.; Buttry, D. A. *J. Am. Chem. Soc.* **1992**, 114, 10085.
- Welford, K. *Opt. Quant. Elec.* **1991**, 23, 1.
- Knoll, W. *MRS Bull.* **1991**, 16, 29.
- Fagerstam, L. G.; O'Shannessy, D. J. In *Handbook of Affinity Chromatography*; Kline, T., Ed.; Marcel Dekker: New York, 1993; Vol. 63, pp 229-52.

Anthony G. Frutos is a graduate student at the University of Wisconsin-Madison. His research focuses on surface chemistry and spectroscopy of modified self-assembled monolayers on gold films and DNA computing on surfaces. Robert M. Corn is a professor at the University of Wisconsin-Madison, and his research focuses on surface chemistry and applying optical spectroscopy to condensed-phase interfaces. Address correspondence about this article to Corn at Department of Chemistry, University of Wisconsin-Madison, 1101 University Ave., Madison, WI 53706 (corn@chem.wisc.edu).